HHS Public Access

Author manuscript

Oncogene. Author manuscript; available in PMC 2021 April 02.

Published in final edited form as:

Oncogene. 2020 November ; 39(48): 7142–7151. doi:10.1038/s41388-020-01487-6.

De novo induction of lineage plasticity from human prostate luminal epithelial cells by activated AKT1 and c-Myc

Oh-Joon Kwon[1], **Li Zhang**[1], **Deyong Jia**[1], **Zhicheng Zhou**[1], **Zhouyihan Li**[2], **Michael Haffner**[3], **John K Lee**[3], **Lawrence True**[4], **Colm Morrissey**[1], **Li Xin**[1,5,6]

[1]Department of Urology, University of Washington, Seattle, WA 98109

[2]Department of Chemistry and Biochemistry, University of Washington, Seattle, WA, 98109

[3]Human Biology Division, Fred Hutch Cancer Research Center, Seattle, WA 98109

[4]Department of Pathology, University of Washington, Seattle, WA 98109

[5]Institute of Stem Cell and Regenerative Medicine, University of Washington, Seattle, WA 98109

Summary

Neuroendocrine prostate cancer (NEPC) is an aggressive variant of prostate cancer that either develops *de novo* or arises from prostate adenocarcinoma as a result of treatment resistance. Although the prostate basal cells have been shown to directly generate tumor cells with neuroendocrine features when transduced with oncogenic signaling, the identity of the cell-of-origin for *de novo* NEPC remains unclear. We show that the TACSTD2^{high} human prostate luminal epithelia cells highly express SOX2 and are relatively enriched in the transition zone prostate. Both TACSTD2^{high} and TACSTD2^{low} luminal cells transduced by activated AKT and c-Myc can form organoids containing versatile clinically relevant tumor cell lineages with regard to the expression of AR and the neuroendocrine cell markers Synaptophysin and Chromogranin A. Tumor organoid cells derived from the TACSTD2^{high} luminal cells are more predisposed to neuroendocrine differentiation along passaging and are relatively more castration-resistant. Knocking down *TACSTD2* and *SOX2* both attenuate neuroendocrine differentiation of tumor organoid cells. This study demonstrates *de novo* neuroendocrine differentiation of the human prostate luminal epithelial cells induced by caAKT and c-Myc and reveals an impact of cellular status on initiation of lineage plasticity.

[6]Corresponding author: Li Xin, Ph.D., University of Washington, 850 Republican Street, Seattle, WA 98109, Phone: 206-543-6551, xin18@uw.edu.

Author contribution

Conception and design: L. Xin and O. Kwon
Development of methodology: L. Xin and O. Kwon
Acquisition of data: O. Kwon, L. Zhang, D. Jia, Z. Zhou, Z, Li, L. True, C. Morrissey, L. Xin
Analysis and interpretation of data: O. Kwon, L. Zhang, D. Jia, M. Haffner, L. Xin
Writing, review, and/or revision of the manuscript: L. Xin and O. Kwon
Administrative, technical, or material support: L. Zhang, D. Jia, J. K. Lee,
Study supervision: L. Xin

Disclosure of Potential Conflicts of Interest

The authors declare no conflict of interest.

Keywords

TACSTD2; cells of origin; castration resistance; neuroendocrine differentiation; lineage plasticity; SOX2

Introduction

Neuroendocrine prostate cancer (NEPC) is an aggressive variant of prostate cancer that either develops *de novo* or arises from patients treated with anti-hormonal therapy for prostate adenocarcinoma (1). Genetic and epigenetic signaling associated with the development of NEPC have been identified, which include loss of function of the tumor suppressor *TP53* and *RB1* (2–4), down regulation of *REST* (5), activation of transcription factors N-MYC (6, 7), ONECUT2 (8, 9), and BRN2 (10), and upregulation of *EZH2* (2, 4). These oncogenic signaling promotes lineage plasticity and reprograms cell identity to induce the emergence of neuroendocrine features (11).

It is largely agreed that NEPC in treatment resistant prostate cancer patients arises via trans-differentiation of adenocarcinoma instigated by therapies (12–14). On the other hand, the identity of the cells of origin for *de novo* NEPC is unclear. Because some of these tumors express the stem cell-associated antigens such as c-KIT and BCL-2 (15), it was hypothesized that their cell-of-origin is multipotent stem cells. The prostate basal cells have been demonstrated to possess the stem cell capacity for multipotent differentiation (16–19). Experimentally, it has been confirmed that the prostate basal cells can generate tumor cells with neuroendocrine features when transduced with oncogenic signaling (20, 21). Nevertheless, recent studies demonstrated that the basal and luminal epithelial cells in adults are independently sustained, which suggests the existence of unipotent progenitor cells in the luminal epithelial lineage (22–26). Recent single-cell analysis and lineage tracing studies have revealed that the mouse Sca-1^{+} luminal cells and the human TACSTD2^{+} luminal cells share molecular feathers (26–30). They both express high levels of SOX2 and TACSTD2, both of which promote lineage plasticity and androgen resistance in human prostate cancer cell line (3, 31). In this study, we provide direct evidence showing *de novo* formation of tumor cells with neuroendocrine features from the human prostate luminal epithelial cells, especially the TACSTD2^{high} luminal cells.

Results

The TACSTD2^{high} human prostate luminal cells highly express SOX2

The TACSTD2-expressing luminal cells have been shown to display a higher progenitor activity (30). We collected 8 benign human prostate specimens from patients underwent radical prostatectomy for the treatment of prostate cancer. The specimens were dissociated into single cells and the Lin^{-}CD326^{+}CD26^{high}CD49f^{low} luminal cells were fractionated into the TACSTD2^{high} and TACSTD2^{low} cells (Fig. 1A). QRT-PCR analysis confirms low expression levels of the basal cell marker *KRT5* and the stromal cell marker *VIM* in the luminal cell fractions, and a higher expression of *TACSTD2* in the TACSTD2^{high} fraction, indicating the successful separation (Fig. 1B). Antigens associated with the luminal

epithelial cells including *KRT8*, *AR*, *HOXB13*, *KLK3*, and *ACPP* are expressed at similar levels between the TACSTD2^{high} and TACSTD2^{low} luminal cells. In contrast, TACSTD2^{high} luminal cells express a higher level of *PSCA*, *SOX2*, and *KRT7*, which is consistent with the observations from the recent single-cell analyses (27, 29).

The human prostate is defined into 4 different zones of which the peripheral zone (PZ) and transition zone (TZ) are the two major zones (32). We performed immunostaining analyses to determine whether the TACSTD2^{high} luminal cells are distributed in different prostatic anatomic locations. We found that there are much more KRT7^{+} (Fig. 1C) and SOX2^{+} luminal cells (Fig. 1D) in human TZ prostate tissues than in PZ tissues. These results corroborate the heterogeneity of the human prostate luminal cells and identify SOX2 and KRT7 as highly expressed antigens in the TACSTD2^{high} luminal cells.

Human prostate luminal cells transduced with caAKT1 and c-Myc exhibit lineage plasticity

Previously, Park *et al* expanded normal human basal and luminal cells in the prostate organoid culture and then transduced cell with a lentivirus expressing a constitutively activated AKT1 (caAKT1) and c-Myc. They show that those organoid cells can form organoids displaying features of human prostate cancer (33). We sought to employ the assay to determine whether both TACSTD2^{high} and TACSTD2^{low} luminal cells can serve as a target for transformation. Briefly, FACS-isolated basal cells, TACSTD2^{high}, and TACSTD2q^{low} luminal cells from benign human prostate tissues were infected with the caAKT1/c-Myc lentiviruses and cultured in the organoid assay. The basal cells are much more efficient than the luminal cells in forming tumor organoids (Fig. 2A) and the organoid size is statistically significantly larger than those in the luminal cell groups (Fig. 2B). Regardless, the organoid-forming activity of the TACSTD2^{high} luminal cells is 3.52-fold higher than that of the TACSTD2^{low} luminal cells (Fig. 2A). But the organoid size is not significantly different (Fig. 2B).

Histologically, the organoids in both luminal groups are either completely or partially filled with cells with no discernible glandular structure and with occasional squamous differentiation (middle panel, Fig. 2C). Immunostaining confirmed that the organoid cells express both pAKT and c-Myc, and are predominantly adenocarcinoma cells expressing KRT8, with rare cells expressing KRT5 mostly in the regions displaying squamous differentiation (Fig. 2D). Organoids that display exclusive squamous differentiation and express KRT5 are extremely rare (less than 0.1%) (Fig. 2E). Immunostaining of AR and SYP (synaptophysin) further reveals a striking heterogeneity inside organoids derived from the TACSTD2^{high} luminal cells. Fig. 2F shows representative images demonstrating the existence of the AR^{+}SYP^{-}, AR^{+}SYP^{+}, AR$^{low/-}$SYP^{-}, and AR$^{low/-}$SYP^{+} cells. Both SYP^{+} and SYP^{-} cells express pAKT (Fig. 2G). Interestingly, the other NE marker, CHGA (chromogranin A), is not expressed (Fig. 2F). The heterogeneity is also observed in the organoids derived from the TACSTD2^{low} luminal cells (Supplementary Fig. 1). The percentage of the SYP^{+} cells in the organoids from the TACSTD2^{low} luminal cells appeared lower, but we were not able to make a definitive conclusion due to very limited number of the primary organoids available for the analysis. In contrast, tumor organoids derived from the basal cells are less heterogeneous. Most of those organoids contain either only KRT5^{+}

cells or KRT5^{+} cells surrounding KRT8^{+} cells, expressing a low or undetectable level of AR and no SYP (Supplementary Fig. 2). These results show that caAKT and c-Myc drive lineage plasticity in both TACSTD2^{high} and TACSTD2^{low} luminal cells.

TACSTD2^{high} luminal cells exhibit higher lineage plasticity along passaging

We passaged the tumor organoids derived from the two types of luminal cell to generate secondary organoids. The secondary organoids are also composed of heterogenous cells including the KRT5^{+} squamous cells (data not shown), AR^{+}SYP^{-}, AR^{+}SYP^{+}, AR$^{low/-}$SYP^{-}, and AR$^{low/-}$SYP^{+} cells (Fig. 3A). The SYP^{+} cells are usually, but not always, located at the outer layer of the organoids, and these cells express SOX2 at a significantly higher level than the remaining cells. Interestingly, CHGA is turned on in 45.3% of the SYP^{+} cells in the secondary organoids, suggesting a continuous neuroendocrine differentiation along passaging. 93.0% of the secondary organoids in the TACSTD2^{high} group contain SYP^{+} NE cells as compared to 39.7% in the TACSTD2^{low} group (Fig. 3B). The enrichment of the NE cells in the TACSTD2^{high} group is confirmed by qRT-PCR analysis of *CHGA*, *SYP*, and *SRRM4*, a gene associated with NE differentiation (Fig. 3C) *SOX2* and *TACSTD2* are also relatively highly expressed in the organoid cells derived from the TACSTD2^{high} group (Supplementary Fig. 3). 72.2% of the AR$^{low/-}$ cells and 28% of the AR^{+} cells proliferated (Ki67^{+}), whereas only 3.9% of the CHGA^{+} cells did (Fig. 3D). Collectively, these results show that the organoid cells derived from the TACSTD2^{high} luminal cells are more predisposed to NE differentiation.

We transplanted approximately 1000 organoids into immunodeficient male SCID/Beige hosts subcutaneously. These organoids formed nodules of 3–5mm in diameter in 4 weeks. The nodules were mainly composed of cells expressing KRT8 and AR. But there were more cells expressing SYP in the nodules outgrown from the TACSTD2^{high} organoids (Supplementary Fig. 4). This demonstrates that these organoid cells are tumorigenic but are not overall aggressive.

TACSTD2 and SOX2 are necessary for NE differentiation of organoid cells

The TACSTD2^{high} luminal cells highly express TACSTD2 and SOX2, both of which have been shown to promote NE differentiation of prostate cancer cells (3, 31). We sought to investigate whether TACSTD2 and SOX2 are necessary for NE differentiation of the organoid cells in our system. Briefly, secondary organoids derived from the TACSTD2^{high} luminal cells were dissociated into single cells and transduced with the lentivirus expressing a scrambled shRNA or shRNAs targeting *TACSTD2* and *SOX2*, respectively. The organoid-forming units in the shTACSTD2 and shSOX2 groups decreased by 50.8% and 42.1%, respectively, as compared to that of the control scrambled shRNA group (Fig. 3E). Downregulation of TACSTD2 and SOX2 by their respective shRNAs in the organoid cells was confirmed by both qRT-PCR and Western blot analyses (Figs. 3F–G). Consistent with a recent report (31), we found that knocking down TACSTD2 decreased expression of SOX2 in the organoid cells (Figs. 3F–G). Meanwhile, suppressing SOX2 also downregulated TACSTD2, suggesting a reciprocal regulation between TACSTD2 and SOX2 (Fig. 3F–G). Interestingly, qRT-PCR analysis revealed that the expression of the NE markers (*CHGA*, *SRRM4*, and *SYP*) all decreased in both the shTACSTD2 and shSOX2 groups (Fig. 3H).

Immunostaining corroborated that the cells expressing CHGA and SYP were significantly reduced in the organoids with TACSTD2 or SOX2 knockdown (Fig. 3I). Similar results were obtained when using different shRNAs (described in the Materials and Methods) targeting *TACSTD2* and *SOX2* (data not shown). Collectively, these results show that both TACSTD2 and SOX2 are critical factors for NE differentiation of the tumor organoid cells.

The organoid cells derived from the TACSTD2^{high} cells are relatively more castration resistant

The human TACSTD2^{high} luminal cells share molecular features with the castration resistant Sca-1^{+} luminal cells in mice (28). To determine the androgen dependency of the tumor organoids, we passaged and cultured organoid cells without testosterone but with enzalutamide. Fig. 4A shows that ablating the AR signaling reduced the organoid-forming units and organoid size in the TACSTD2^{low} group but did not significantly affect those of the TACSTD2^{high} group. Immunostaining showed that nuclear AR staining was almost ablated upon enzalutamide treatment, corroborating that AR signaling was efficiently suppressed (Fig. 4B). Immunostaining of Ki67 and CC3 indicates that the decreased organoid size was a result of both reduced proliferation and increased apoptosis (Fig. 4C). Interestingly, ablating androgen signaling did not enhance NE differentiation as determined by qRT-PCR analysis of the NE-associated genes (Fig. 4D). These results show that the organoid cells derived from the TACSTD2^{high} cells are relatively more castration resistant as compared to those from the TACSTD2^{low} cells.

Discussion

Lineage plasticity is a biological process through which cells take on an alternative morphological, phenotypic or epigenetic state (11). It is a strategy that cells utilize to adapt to their environment during normal development. Recent studies in melanoma, lung cancer and prostate cancer also demonstrated it as a mechanism through which tumor cells acquire therapeutic resistance. For example, to outwit the anti-androgen therapies, prostate adenocarcinoma cells initially boost the androgen signaling using versatile mechanisms such as AR mutations and amplifications, but eventually evolve to AR^{low} tumors, amphicrine tumors composed of cells coexpressing AR and the NE genes, double-negative tumors (AR^{-}/NE^{-}), AR negative NE tumors, basal squamous tumors, or a mixture of these types of tumors (34). Interestingly, the tumor organoids derived from the prostate luminal cells transduced by caAKT1 and c-Myc contain all types of the tumor cells observed in the clinic. This observation supports the trans-differentiation of the adenocarcinoma to NEPC.

We also showed that there is more NE differentiation in the organoids derived from the TACSTD2^{high} luminal cells. The TACSTD2^{high} luminal cells express a relatively higher level of SOX2 (Fig. 1B). Both TACSTD2 and SOX2 have been shown to promote NE differentiation of prostate cancer cells (3, 31). In addition, TACSTD2-expressing luminal cells have been shown to display higher progenitor activities (30). Therefore, the TACSTD2^{high} luminal cells are probably at a cellular state that is more susceptible to be reprogramed toward the NE lineage given an optimal change in the environmental and

genetic cues. It is tempting to hypothesize that these cells represent one cell-of-origin for the aggressive prostate cancer.

Lineage plasticity is rarely seen in primary prostate cancer, thereby is considered as an anti-androgen therapy-induced event. In addition, N-Myc, but not c-Myc, is considered associated with NE differentiation during human prostate cancer progression (6, 20). However, we were able to see all types of clinically relevant tumor cell lineages in the organoids outgrown from the human luminal cells transduced with caAKT and c-Myc in the presence of testosterone. It is possible that, unlike the tumor organoid cells, prostate cancer cells in patients are usually already treated before they can exhibit spontaneous lineage plasticity. Alternatively, the signaling presented in the organoid assay, such as the Wnt and FGF signaling (35), primes the luminal cells for reprograming and facilitates lineage plasticity in different genetic contexts. Future study will interrogate molecular mechanisms that regulate the capacities of the tumor derived from the TACSTD2^{high} luminal cells for castration resistance and NE differentiation.

Materials and Methods

Human specimens

The human PZ and TZ prostate specimens used in this study were obtained from patients underwent radical prostatectomy for the treatment of prostate cancer at the Michael E. DeBakey Veteran Medical Center at Houston, Texas, and the University of Washington at Seattle with IACUC protocols approved by respective Institutional Review Boards. Collected specimens were fixed in 10% formalin at 4°C for 12 hours. Tissue sections were reviewed by Drs. Michael Ittmann and Michael Haffner to confirm that the areas of specimens used in the study were devoid of tumor or benign prostatic hyperplasia. Immunostaining using antibodies against CK5 and TP63 was also performed to confirm the absence of tumor.

Mice

The SCID/Beige mice were purchased from Charles River (Wilmington, MA). All the mice used in this study received humane care in compliance with the principles stated in the Guide for the Care and Use of Laboratory Animals, NIH Publication, 1996 edition, and the protocols were approved by the Institutional Animal Care Committee at Baylor College of Medicine and the University of Washington.

Preparation of dissociated human prostate single cells

Human prostate tissues were chopped into 2–3 mm-long pieces and incubated in 5mg/ml collagenase type II/ advanced DMEM/F12 (1 ml per 50 mg of prostate tissue) with 10 μM of Y-27632 (STEMCELL technologies) for 5–12 hours. Tissues were pelleted, resuspended, and incubated in chilled 0.25% Trypsin-EDTA for 5 min. Thereafter, human prostate tissues were pelleted, resuspended in Dispase (Invitrogen, Carlsbad, CA, 5 mg/mL) and DNase I (Roche Applied Science, Indianapolis, IN, 1 mg/mL), and pipetted vigorously to dissociate cell clumps. Dissociated cells were then passed through 70 μm cell strainers (BD Biosciences, San Jose, CA) to obtain single cells.

Flow cytometry and cell sorting

Dissociated single human prostate cells were incubated with florescence conjugated antibodies on ice for 30 minutes. After washing with 10% FBS-containing RPMI1640, FACS analyses and sorting were performed using the BD LSR II, and Aria II (BD Biosciences, San Jose, CA). Gating was set up using fluorescence minus one. Antibodies for FACS analysis and sorting are listed in Supplementary Table 1.

RNA isolation and quantitative RT–PCR

Total RNA was extracted using Nucleospin RNA XS or XS plus Kit (Macherey-Nagel, Bethlehem, PA). RNA was reverse transcribed to cDNA using iScript™ Reverse Transcription Supermix (Bio-Rad, Hercules, CA). QRT-PCR was performed using SYBR Green system (Bio-Rad) and detected on a StepOne plus Real-Time PCR system (Applied Biosystems, Foster City, CA). Primers for target genes are listed in Supplementary Table 2.

Lentivirus preparation and infection

The lentiviral vectors expressing c-Myc and caAKT are as described previously (33, 36). The shRNAs were cloned into the pLKO.1 vector as described at https://www.addgene.org/protocols/plko/#B. The shRNA sequences are as below: the scrambled shRNA (CCGGCCTAAGGTTAAGTCGCCCTCGCTCGAGCGAGGGCGACTTAA CCTTAGGTTTTTG), the *TACSTD2* shRNAs (CCGGGAGAAAGGAACCGAGCTTGTACTCGAGTACAAGCTCGGTTCCTTTCTCTTT TTG and CCGGCGTGGACAACG ATGGCCTCTACTCGAGTAGAGGCCATCGTTGTCCACGTTTTTG), the *SOX2* shRNAs (CCGGCGAGATAAACATGGCAATCAACTCGAGTTGA TTGCCATGTTTATCTCGTTTTTG, and CCGGCAGCTCGCAGACCTACATGAACTCGAGTTCATGTAGGTCTGCGAGCTGTTT TTG). The lentiviruses preparation and titration and infection of FACS-isolated prostate cells were as described previously (36).

Human prostate organoid assay

FACS-isolated human prostate basal, TACSTD2^{low} luminal, and TACSTD2^{high} luminal cells were infected by lentiviruses at an M.O.I of 50 and cultured in Corning® Matrigel® Basement Membrane Matrix with advanced DMEM/F12 supplemented with B27 (Life technologies), 10 mM HEPES, glutamax (Life technologies), penicillin/streptomycin, and the following growth factors: 5 ng/ml EGF (Peprotech, Rocky Hill, NJ), 5 ng/ml FGF2 (Peprotech, Rocky Hill, NJ), 10 ng/ml FGF (Peprotech, Rocky Hill, NJ), 500 ng/ml R-spondin1 (Peprotech, Rocky Hill, NJ), 100 ng/ml Noggin (Peprotech, Rocky Hill, NJ), 500 nM of A83–01 (Tocris, Ellisville, MO), Prostaglandin E2 (1 μM), Nicotinamide (10 mM), 10 μm Y-27632 (Tocris, Ellisville, MO), and 1 nM of DHT (Sigma, St. Louis, MO).

To collect organoids for histological and IHC analyses, 1 mg/mL dispase (Invitrogen, Carlsbad, CA) was added and incubated for 1 hour at 37 °C. Organoids were then fixed using 10% formalin for 10 minutes and resuspended in 50 μl of Richard-Allan Scientific™ HistoGel™ Specimen Processing Gel (Thermo Fisher) for preparation of paraffin embedded blocks. To passage organoids, organoids released from Matrigel by dispase were treated with

0.05% Trypsin-EDTA for 5 min at room temperature and passed through 28-Gauge insulin syringe to obtain single cells. For in vivo transplantation, organoids released from Matrigel were resuspended in 50% Matrigel in PBS and injected subcutaneously into 8–10 week old male SCID/Beige mice.

Western blot

Collected organoids were lysed in RIPA buffer (20mM Tris-HCl, pH 7.5, 150mM NaCl, 1mM Na2EDTA, 1mM EGTA, 1% NP-40, 1% sodium deoxycholate, 2.5mM sodium pyrophosphate, 1mM b-glycerophosphate and 1mM Na_3VO_4) with protease inhibitors and phosphatase inhibitors (Roche Applied Science). Protein concentrations were determined by a Bradford Assay kit (Bio-Rad). Protein was separated by 10% SDS/PAGE and transferred onto a polyvinylidene difluoride (PVDF) membrane (Amersham Biosciences, Arlington Heights, IL). The membrane was blocked in 5% skim milk, and subsequently incubated with primary antibodies listed in Supplementary Table 3 at 4°C overnight followed by incubation with peroxidase-conjugated goat anti-mouse IgG or goat anti-rabbit IgG (Jackson ImmunoResearch, Inc., West Grove, PA), and developed with Pierce ECL reagent (Thermo Scientific, Rockford, IL).

Histology and Immunostaining

Human prostate tissues were fixed by 10% buffered formalin and paraffin embedded. H&E staining and immunofluorescence staining were performed using standard protocols on 5-μm paraffin sections. Slides were incubated with 5% normal goat serum (Vector Labs, Burlingame, CA) and with primary antibodies diluted in 3% normal goat serum overnight at 4°C. Information for primary antibodies is listed in Supplementary Table 3. Slides were then incubated with secondary antibodies (diluted 1:500 in 0.05% tween 20 in PBS) labeled with Alexa Fluor 488, 568, 594, or 633 (Invitrogen/Molecular Probes, Eugene, OR). Sections were counterstained with NucBlue™ Fixed Cell ReadyProbes™ Reagent (Thermo Fisher). Immuno-fluorescence staining was imaged using Leica DM4B fluorescent microscope or LeicaSP8 confocal microscope (Leica Microsystems, Wetzlar, Germany). All representative images were quantified using the Image J software.

Statistical analyses

All experiments were performed using prostate specimens from 3–22 human subjects in independent experiments. Data are presented as mean ± SD or mean ± SEM. Statistical analysis was done using Microsoft Excel or GraphPad 8. Probability < 0.05 was considered the statistical significance threshold.

Supplementary Material

Refer to Web version on PubMed Central for supplementary material.

Acknowledgements

This work is supported by R01CA190378, R01DK092202, and R01DK107436 (L.X.).

References

1. Conteduca V, Oromendia C, Eng KW, Bareja R, Sigouros M, Molina A, et al. Clinical features of neuroendocrine prostate cancer. Eur J Cancer. 2019;121:7–18. Epub 2019/09/17. [PubMed: 31525487]
2. Ku SY, Rosario S, Wang Y, Mu P, Seshadri M, Goodrich ZW, et al. Rb1 and Trp53 cooperate to suppress prostate cancer lineage plasticity, metastasis, and antiandrogen resistance. Science. 2017;355(6320):78–83. Epub 2017/01/07. [PubMed: 28059767]
3. Mu P, Zhang Z, Benelli M, Karthaus WR, Hoover E, Chen CC, et al. SOX2 promotes lineage plasticity and antiandrogen resistance in TP53- and RB1-deficient prostate cancer. Science. 2017;355(6320):84–8. Epub 2017/01/07. [PubMed: 28059768]
4. Beltran H, Prandi D, Mosquera JM, Benelli M, Puca L, Cyrta J, et al. Divergent clonal evolution of castration-resistant neuroendocrine prostate cancer. Nat Med. 2016;22(3):298–305. Epub 2016/02/09. [PubMed: 26855148]
5. Lapuk AV, Wu C, Wyatt AW, McPherson A, McConeghy BJ, Brahmbhatt S, et al. From sequence to molecular pathology, and a mechanism driving the neuroendocrine phenotype in prostate cancer. The Journal of pathology. 2012;227(3):286–97. Epub 2012/05/04. [PubMed: 22553170]
6. Dardenne E, Beltran H, Benelli M, Gayvert K, Berger A, Puca L, et al. N-Myc Induces an EZH2-Mediated Transcriptional Program Driving Neuroendocrine Prostate Cancer. Cancer Cell. 2016;30(4):563–77. Epub 2016/10/12. [PubMed: 27728805]
7. Beltran H, Rickman DS, Park K, Chae SS, Sboner A, MacDonald TY, et al. Molecular characterization of neuroendocrine prostate cancer and identification of new drug targets. Cancer discovery. 2011;1(6):487–95. Epub 2012/03/06. [PubMed: 22389870]
8. Guo H, Ci X, Ahmed M, Hua JT, Soares F, Lin D, et al. ONECUT2 is a driver of neuroendocrine prostate cancer. Nature communications. 2019;10(1):278 Epub 2019/01/19.
9. Rotinen M, You S, Yang J, Coetzee SG, Reis-Sobreiro M, Huang WC, et al. ONECUT2 is a targetable master regulator of lethal prostate cancer that suppresses the androgen axis. Nat Med. 2018;24(12):1887–98. Epub 2018/11/28. [PubMed: 30478421]
10. Bishop JL, Thaper D, Vahid S, Davies A, Ketola K, Kuruma H, et al. The Master Neural Transcription Factor BRN2 Is an Androgen Receptor-Suppressed Driver of Neuroendocrine Differentiation in Prostate Cancer. Cancer discovery. 2017;7(1):54–71. Epub 2016/10/28. [PubMed: 27784708]
11. Beltran H, Hruszkewycz A, Scher HI, Hildesheim J, Isaacs J, Yu EY, et al. The Role of Lineage Plasticity in Prostate Cancer Therapy Resistance. Clin Cancer Res. 2019;25(23):6916–24. Epub 2019/08/01. [PubMed: 31363002]
12. Davies AH, Beltran H, Zoubeidi A. Cellular plasticity and the neuroendocrine phenotype in prostate cancer. Nature reviews Urology. 2018;15(5):271–86. Epub 2018/02/21. [PubMed: 29460922]
13. Zou M, Toivanen R, Mitrofanova A, Floch N, Hayati S, Sun Y, et al. Transdifferentiation as a Mechanism of Treatment Resistance in a Mouse Model of Castration-Resistant Prostate Cancer. Cancer discovery. 2017;7(7):736–49. Epub 2017/04/16. [PubMed: 28411207]
14. Lin D, Wyatt AW, Xue H, Wang Y, Dong X, Haegert A, et al. High fidelity patient-derived xenografts for accelerating prostate cancer discovery and drug development. Cancer Res. 2014;74(4):1272–83. Epub 2013/12/21. [PubMed: 24356420]
15. Yao JL, Madeb R, Bourne P, Lei J, Yang X, Tickoo S, et al. Small cell carcinoma of the prostate: an immunohistochemical study. Am J Surg Pathol. 2006;30(6):705–12. Epub 2006/05/26. [PubMed: 16723847]
16. Goldstein AS, Huang J, Guo C, Garraway IP, Witte ON. Identification of a cell of origin for human prostate cancer. Science. 2010;329(5991):568–71. Epub 2010/07/31. [PubMed: 20671189]
17. Leong KG, Wang BE, Johnson L, Gao WQ. Generation of a prostate from a single adult stem cell. Nature. 2008;456(7223):804–8. Epub 2008/10/24. [PubMed: 18946470]
18. Collins AT, Habib FK, Maitland NJ, Neal DE. Identification and isolation of human prostate epithelial stem cells based on alpha(2)beta(1)-integrin expression. Journal of cell science. 2001;114(Pt 21):3865–72. [PubMed: 11719553]

19. Lawson DA, Xin L, Lukacs RU, Cheng D, Witte ON. Isolation and functional characterization of murine prostate stem cells. Proc Natl Acad Sci U S A. 2007;104(1):181–6. [PubMed: 17185413]
20. Lee JK, Phillips JW, Smith BA, Park JW, Stoyanova T, McCaffrey EF, et al. N-Myc Drives Neuroendocrine Prostate Cancer Initiated from Human Prostate Epithelial Cells. Cancer Cell. 2016;29(4):536–47. Epub 2016/04/07. [PubMed: 27050099]
21. Park JW, Lee JK, Sheu KM, Wang L, Balanis NG, Nguyen K, et al. Reprogramming normal human epithelial tissues to a common, lethal neuroendocrine cancer lineage. Science. 2018;362(6410):91–5. Epub 2018/10/06. [PubMed: 30287662]
22. Choi N, Zhang B, Zhang L, Ittmann M, Xin L. Adult murine prostate basal and luminal cells are self-sustained lineages that can both serve as targets for prostate cancer initiation. Cancer Cell. 2012;21(2):253–65. Epub 2012/02/22. [PubMed: 22340597]
23. Wang ZA, Mitrofanova A, Bergren SK, Abate-Shen C, Cardiff RD, Califano A, et al. Lineage analysis of basal epithelial cells reveals their unexpected plasticity and supports a cell-of-origin model for prostate cancer heterogeneity. Nature cell biology. 2013;15(3):274–83. Epub 2013/02/26. [PubMed: 23434823]
24. Lu TL, Huang YF, You LR, Chao NC, Su FY, Chang JL, et al. Conditionally ablated Pten in prostate basal cells promotes basal-to-luminal differentiation and causes invasive prostate cancer in mice. Am J Pathol. 2013;182(3):975–91. Epub 2013/01/15. [PubMed: 23313138]
25. Liu J, Pascal LE, Isharwal S, Metzger D, Ramos Garcia R, Pilch J, et al. Regenerated luminal epithelial cells are derived from preexisting luminal epithelial cells in adult mouse prostate. Mol Endocrinol. 2011;25(11):1849–57. Epub 2011/09/24. [PubMed: 21940754]
26. Kwon OJ, Zhang L, Xin L. Stem Cell Antigen-1 Identifies a Distinct Androgen-Independent Murine Prostatic Luminal Cell Lineage with Bipotent Potential. Stem Cells. 2015 Epub 2015/09/30.
27. Karthaus WR, Hofree M, Choi D, Linton EL, Turkekul M, Bejnood A, et al. Regenerative potential of prostate luminal cells revealed by single-cell analysis. Science. 2020;368(6490):497–505. Epub 2020/05/02. [PubMed: 32355025]
28. Kwon OJ, Choi JM, Zhang L, Jia D, Li Z, Zhang Y, et al. The Sca-1(+) and Sca-1(−) mouse prostatic luminal cell lineages are independently sustained. Stem Cells. 2020 Epub 2020/07/07.
29. Joseph DB, Henry GH, Malewska A, Iqbal NS, Ruetten HM, Turco AE, et al. Urethral luminal epithelia are castration-insensitive cells of the proximal prostate. Prostate. 2020;80(11):872–84. Epub 2020/06/05. [PubMed: 32497356]
30. Crowell PD, Fox JJ, Hashimoto T, Diaz JA, Navarro HI, Henry GH, et al. Expansion of Luminal Progenitor Cells in the Aging Mouse and Human Prostate. Cell reports. 2019;28(6):1499–510 e6. Epub 2019/08/08. [PubMed: 31390564]
31. Hsu EC, Rice MA, Bermudez A, Marques FJG, Aslan M, Liu S, et al. Trop2 is a driver of metastatic prostate cancer with neuroendocrine phenotype via PARP1. Proc Natl Acad Sci U S A. 2020 Epub 2020/01/15.
32. McNeal JE, Redwine EA, Freiha FS, Stamey TA. Zonal distribution of prostatic adenocarcinoma. Correlation with histologic pattern and direction of spread. Am J Surg Pathol. 1988;12(12):897–906. Epub 1988/12/01. [PubMed: 3202246]
33. Park JW, Lee JK, Phillips JW, Huang P, Cheng D, Huang J, et al. Prostate epithelial cell of origin determines cancer differentiation state in an organoid transformation assay. Proc Natl Acad Sci U S A. 2016;113(16):4482–7. Epub 2016/04/05. [PubMed: 27044116]
34. Labrecque MP, Coleman IM, Brown LG, True LD, Kollath L, Lakely B, et al. Molecular profiling stratifies diverse phenotypes of treatment-refractory metastatic castration-resistant prostate cancer. The Journal of clinical investigation. 2019;130:4492–505. Epub 2019/07/31.
35. Karthaus WR, Iaquinta PJ, Drost J, Gracanin A, van Boxtel R, Wongvipat J, et al. Identification of multipotent luminal progenitor cells in human prostate organoid cultures. Cell. 2014;159(1):163–75. Epub 2014/09/10. [PubMed: 25201529]
36. Xin L, Teitell MA, Lawson DA, Kwon A, Mellinghoff IK, Witte ON. Progression of prostate cancer by synergy of AKT with genotropic and nongenotropic actions of the androgen receptor. Proc Natl Acad Sci U S A. 2006;103(20):7789–94. Epub 2006/05/10. [PubMed: 16682621]

Significance

This study provides direct evidence that the luminal epithelial cells could be a cell-of-origin for *de novo* NEPC. The luminal cell-derived tumor organoids represent a novel research platform for mechanistic study of lineage plasticity.

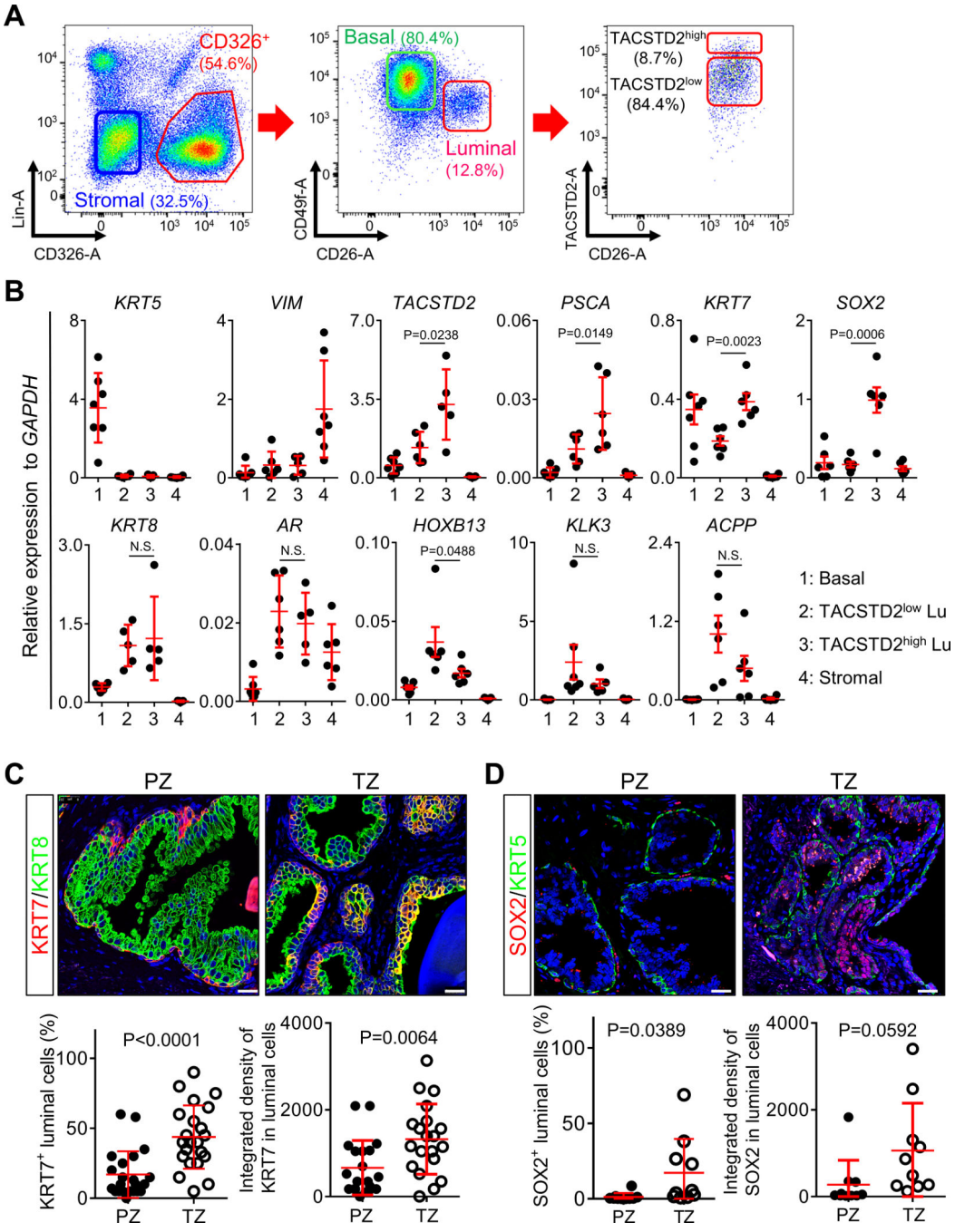

Figure 1. TACSTD2^{high} luminal cells highly express SOX2 and enriched in human prostate transition zone.

(A) FACS plots to separate human prostate basal (Lin^{-}CD326^{+}CD26^{low}CD49f^{high}), TACSTD2^{low} luminal (Lin^{-}CD326^{+}CD26^{high}CD49f^{low}TACSTD2^{low}), TACSTD2^{high} luminal (Lin^{-}CD326^{+} CD26^{high}CD49f^{low}TACSTD2^{high}) and stromal cells (Lin^{-}CD326^{-}). Lin: the mixture of CD45, CD31, and CD235a antibodies. (B) Dot plots show means ± SD of expression of 11 genes in FACS-isolated human prostate cell lineages by qRT-PCR. N=5–7. Lu: luminal. N.S.: no significant. (C) Co-immunostaining of KRT7/KRT8 in benign human prostate PZ and TZ prostate. Scale bars:50 μm. Dot plots shows means ± SD of

percentages of $KRT7^+$ cells (left plot) and quantification of integrated density of immunostaining (right plot). Each dot shows average value from 3–5 representative images of each donor. PZ: peripheral zone. TZ: transition zone. N=22. (D) Co-immunostaining of SOX2/KRT5 in benign human PZ and TZ. Scale bars:50 μm. Dot plots shows means ± SD of percentages of $SOX2^+$ cells (left plot) and quantification of integrated density of immunostaining (right plot). Each dot shows average value from 3–5 representative images of each donor. PZ: peripheral zone. TZ: transition zone. N=10.

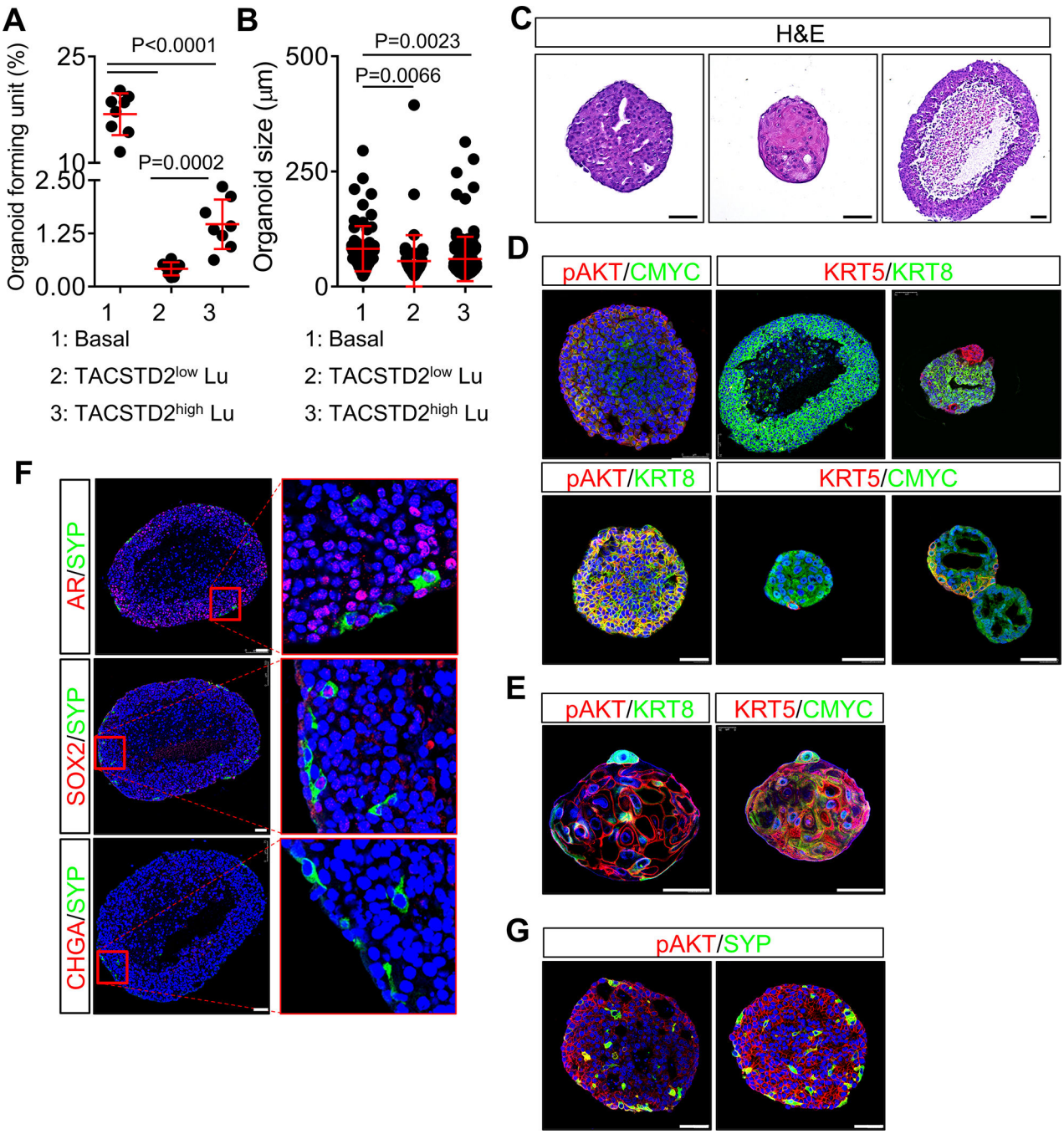

Figure 2. Human prostate luminal cells overexpressing caAKT1 and c-MYC exhibit lineage plasticity in prostate organoid assay.

(A) Dot plot shows means ± SD of organoid forming units of basal, TACSTD2^{high} and TACSTD2^{low} luminal (Lu) cells. Dot represents result from individual donor (N=8). (B) Dot plot shows means ± SD of organoid size. Dots represent results from 50–125 organoids from 8 different donors. (C) H&E staining of primary organoids. Scale bars:25 μm. (D) Co-immunostaining of pAKT/cMYC, KRT5/KRT8, pAKT/KRT8 and KRT5/cMYC of primary organoids. Scale bars=50 μm. (E) Co-immunostaining of pAKT/KRT8 and KRT5/cMYC of primary organoid with squamous differentiation. Scale bars=50 μm. (F) Co-immunostaining

of AR/SYP, SOX2/SYP, and CHGA/SYP of primary organoids. Scale bars: 50 μm. (G) Co-immunostaining of pAKT/SYP in primary organoids. Scale bars: 50 μm.

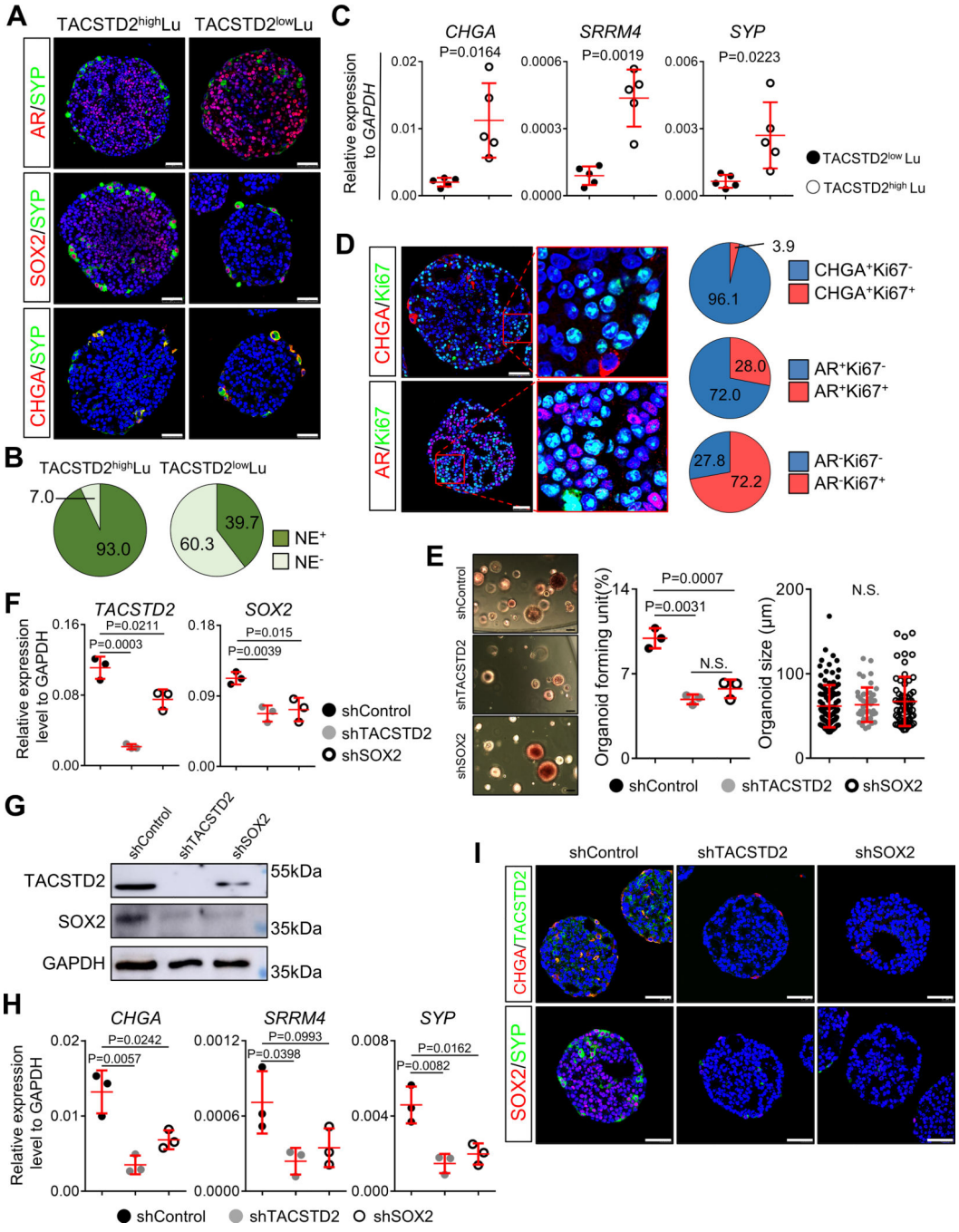

Figure 3. TACSTD2^{high} luminal cells are more predisposed to NE differentiation dependent of TACSTD2 and SOX2.

(A) Co-immunostaining of AR/SYP, SOX2/SYP, and CHGA/SYP of secondary TACSTD2^{high} and TACSTD2^{low} organoids. Scale bars: 50 μm. (B) Pie chart shows quantification of organoids containing NE cells. (C) Dot plots show means ± SD of expression of *CHGA, SRRM4*, and *SYP* in human prostate tumor secondary organoids by qRT-PCR. Results were from 5 experiments using cells from different donors. (D) Co-immunostaining of CHGA/Ki67 and AR/Ki67 in secondary organoids. Pie charts show quantification of Ki67^{+} cells. (E) Transillumination images with overlaid red fluorescence

show day-12 organoids derived from cells transduced with lentivirus expressing red fluorescent protein (RFP) with scrambled shRNA (shControl) or shRNAs targeting *TACSTD2* (shTACSTD2) and *SOX2* (shSOX2). Dot plot in the middle shows means ± SD of organoid forming unit from 3 independent experiments. Dot plot on the right shows means ± SD of organoid size. Dots represent 45–110 organoids from 3 independent experiments using cells from different donors. Scale Bars: 50 μm. N.S.: no significance. (F) Dot plots show means ± SD of expression of *TACSTD2* and *SOX2* by qRT-PCR in organoids derived from cells transduced with lentivirus expressing shControl, shTACSTD2, and shSOX2, respectively. N=3. (G) Western blot shows expression of TACSTD2 and SOX2 in organoids derived from cells transduced with shControl, shTACSTD2, and shSOX2-expressing lentivirus, respectively. (H) Dot plots show means ± SD of expression of *CHGA, SRRM4*, and *SYP* by qRT-PCR in organoids derived from cells transduced with lentivirus expressing shControl, shTACSTD2, and shSOX2, respectively (N=3). (I) Co-immunostaining of CHGA/TACSTD2 and SOX2/SYP in organoids derived from cells transduced with lentivirus expressing shControl, shTACSTD2, and shSOX2, respectively. Scale bars: 50 μm.

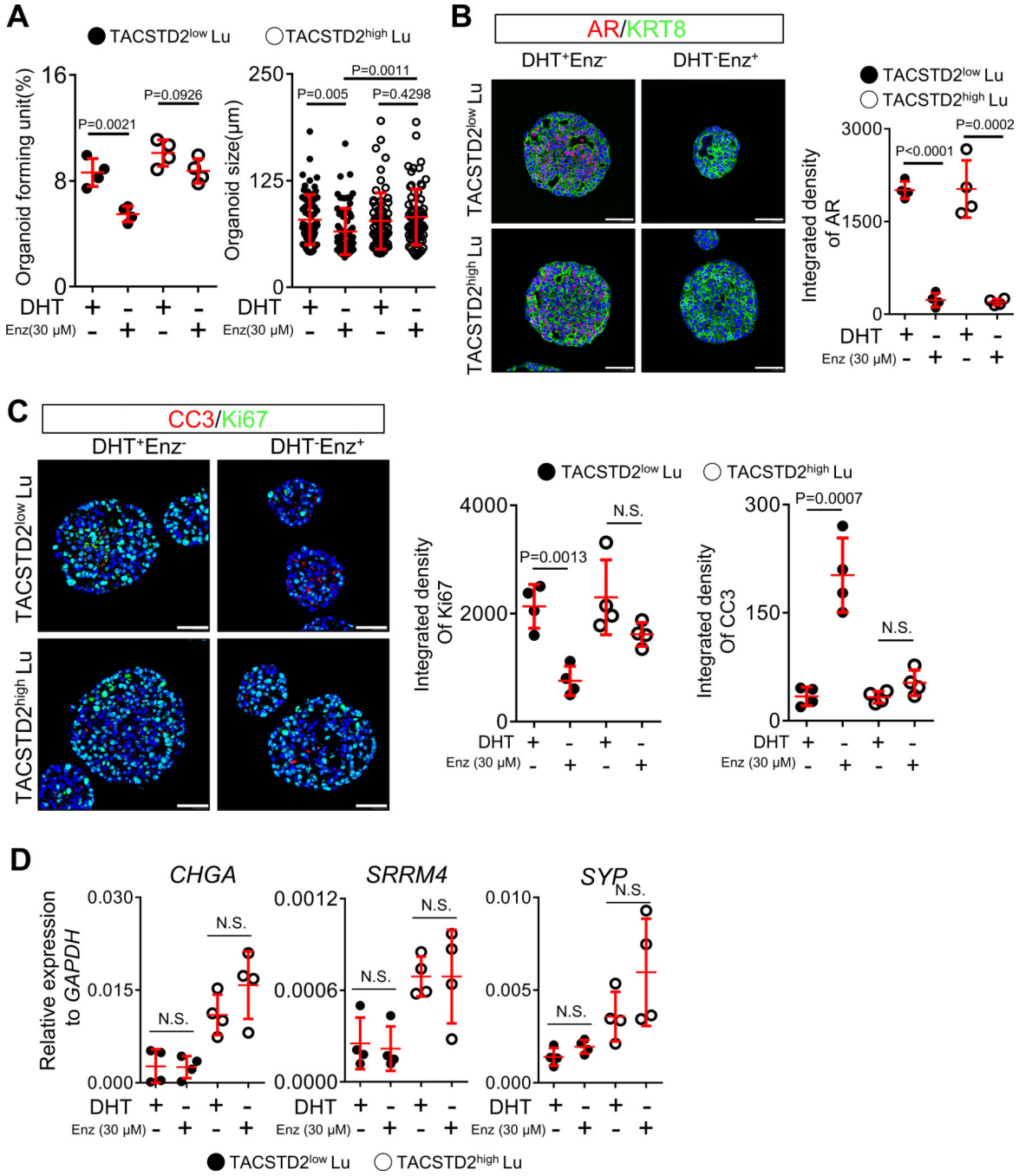

Figure 4. Prostate tumor organoids from TACSTD2^{high} luminal cells show androgen resistance.

(A) Dot plot on the left shows means ± SD of organoid forming unit of TACSTD2^{high} and TACSTD2^{low} cultures. Results were from 4 independent experiments from different donor cells. Dot plot on the right shows means ± SD of organoid size. Dots represent 63–71 organoids from 4 experiments using different donor cells. DHT: dihydrotestosterone; Enz: enzalutamide. N.S.: no significant. Lu: luminal. (B) Co-immunostaining of AR/KRT8 of TACSTD2^{high} and TACSTD2^{low} organoids with DHT or with Enz. Dot plot shows means ± SD of integrated density of AR staining. Each dot represents average value from 4

experiments using different donor cells. Average value was obtained by measuring staining intensity from 22–35 representative organoids in each experiment. Scale bars:50 μm. (C) Co-immunostaining of CC3/Ki67 of organoids. Scale bars:50 μm. Dot plots show means ± SD of integrated density of staining of Ki67 (left) and CC3 (right). Each dot represents average value from 4 experiments using different donor cells. Average value was obtained by measuring staining intensity from 44–50 representative organoids in each experiment. Scale bars:50 μm. N.S.: no significance (D) Dot plots show means ± SD of expression level of 3 NE genes by qRT-PCR in TACSTD2^{high} and TACSTD2^{low} organoids. Results were from 4 experiments using different donor cells.